

A fast microfluidic mixer based on acoustically driven sidewall-trapped microbubbles

Daniel Ahmed · Xiaole Mao · Bala Krishna Juluri ·
Tony Jun Huang

Received: 26 January 2009 / Accepted: 30 March 2009 / Published online: 25 April 2009
© Springer-Verlag 2009

Abstract Due to the low Reynolds number associated with microscale fluid flow, it is difficult to rapidly and homogeneously mix two fluids. In this letter, we report a fast and homogenized mixing device through the use of a bubble-based microfluidic structure. This micromixing device worked by trapping air bubbles within the pre-designed grooves on the sidewalls of the channel. When acoustically driven, the membranes (liquid/air interfaces) of these trapped bubbles started to oscillate. The bubble oscillation resulted in a microstreaming phenomenon—strong pressure and velocity fluctuations in the bulk liquid, thus giving rise to fast and homogenized mixing of two side-by-side flowing fluids. The performance of the mixer was characterized by mixing deionized water and ink at different flow rates. The mixing time was measured to be as small as 120 ms.

Keywords Microfluidics · Rapid mixing · Bubble-trap · Acoustic microstreaming

Electronic supplementary material The online version of this article (doi:10.1007/s10404-009-0444-3) contains supplementary material, which is available to authorized users.

D. Ahmed · X. Mao · B. K. Juluri · T. J. Huang (✉)
Department of Engineering Science and Mechanics,
Pennsylvania State University, University Park, PA 16802, USA
e-mail: junhuang@psu.edu

X. Mao · T. J. Huang
Department of Bioengineering, Pennsylvania State University,
University Park, PA 16802, USA

1 Introduction

The last two decades has witnessed the growing popularity of microfluidics in a wide variety of applications, such as biomedical analysis, drug delivery, chemical synthesis, and enzyme reactions (Ho and Tai 1998; Whitesides 2006; Li 2008). The promise of microfluidic systems lies in their capability to utilize minute quantities of reagents to carry out reactions and analysis with high resolution in a time and cost-efficient manner (Sannomiya et al. 2008). These microfluidic systems often require components that can rapidly and effectively mix different solutions in microscale (Law and Khoo 2002; Chen and Meiners 2004; Ottino and Wiggins 2004; Lam et al. 2005; Chang and Yang 2007; Lee et al. 2007). To date, a number of micromixing methods have been demonstrated, such as chaotic advection (Stroock et al. 2002; Chen and Meiners 2004; Lee et al. 2007; Lin et al. 2007), hydrodynamic focusing (Park et al. 2006; Mao et al. 2007a), electrokinetically driven mixing (Erickson and Li 2002; Lee et al. 2004; Wu and Li 2008), and thermally (Tsai and Lin 2002) and optically (Hellman et al. 2007) induced mixing. Among these methods, acoustic-based mixers have garnered great interest due to their non-invasive nature (Shi et al. 2008) and simple, inexpensive fabrication procedures and instrumentations. Yaralioglu et al. (2004) demonstrated a mixing device based on an integrated ultrasonic transducer. The ultrasound generated pressure fluctuations in liquids and disturbed the laminar flow pattern to facilitate mixing. Mixing via chaotic advection induced by the interaction of acoustic waves with liquids enclosed between two substrates is also demonstrated (Frommelt et al. 2008).

It has been shown that the performance of acoustic micromixing can be further improved by introducing microbubbles into the mixing device. Due to the coupling

of bubbles with acoustic waves, the bubbles act as focusing agents (Marmottant and Hilgenfeldt 2004) of the acoustic energy and thus significantly enhance the mixing performance. Liu et al. (2002) demonstrated this phenomenon using a chamber that consists of multiple bubbles and a piezo transducer disk bonded at the chamber backside to generate acoustic waves. Mixing was observed as these bubbles were driven by the transducer. Despite their promise, the current acoustic-based mixing methods are limited by their slow mixing speed—it takes these methods a few seconds to tens of seconds to achieve homogenous mixing—and thus are not suitable for applications where fast mixing is needed, such as in enzymatic reactions (Song and Ismagilov 2003).

In this communication, we demonstrated rapid and homogenous mixing of fluids through acoustic streaming phenomenon around microbubbles trapped in the sidewall grooves. The mixing time was as low as 120 ms. To the best of our knowledge, this is the fastest mixing speed achieved in acoustic-based mixing devices. The experimental setup is shown in Fig. 1a. A single-layer Y-shaped polydimethylsiloxane (PDMS) microchannel with two inlets and one outlet was fabricated. The channel featured rectangular grooves on the sidewalls designed with alternate spacing. As liquid was injected into the inlets, bubbles were trapped inside the sidewall grooves due to surface tension (Fig. 1b, c). The bubble trapping process is shown in Video 1 in the Supporting Information. The trapped air bubbles were externally excited by acoustic energy from a piezo transducer, causing the membranes (air/liquid interfaces) to oscillate. As a result frictional force was developed between the boundary of the bubble and the surrounding medium (Leighton 1994). This oscillation generated pressure and velocity fluctuations in the surrounding liquid, resulting in a phenomenon known as microstreaming (Tho et al. 2007). The streaming pattern was represented in Fig. 1d by a pair of counter-rotating vortices. The streaming effects drastically perturbed the bulk fluid flow, broke the laminar fluid interface (Mao et al. 2007b), and enhanced the mass transport between the two fluids, thus making fast and homogenous mixing possible.

2 Theory

The streaming phenomenon is most prominent when the bubbles are driven at the natural frequency. The natural frequency f (unit: kHz) of an acoustically oscillated spherical bubble can be approximated by small amplitude behavior of Rayleigh–Plesset equation (Leighton 1994),

$$f^2 = \frac{1}{4\rho\pi^2 a^2} \left\{ 3\kappa \left(p_o + \frac{2\sigma}{a} \right) - \frac{2\sigma}{a} \right\}, \quad (1)$$

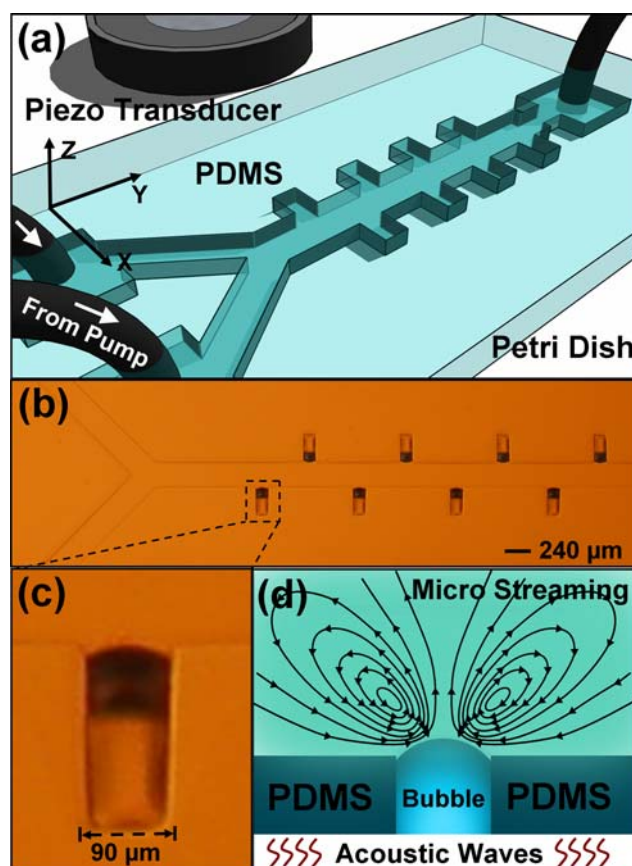


Fig. 1 **a** Schematic of the experimental setup. The microfluidic channel and the piezo transducer was bonded onto a Petri dish and placed adjacent to each other. The polyethylene tubings from the channel were connected to syringe pumps (marked as *white arrows*). The acoustic transducer was driven by a function generator and the whole setup was mounted on an optical microscope stage. **b** Deionized water was injected into the channel, thus trapping air bubbles on the sidewalls of the channel. **c** Magnified image of a single bubble trapped in the sidewall groove. **d** Schematic of the microstreaming phenomenon around an acoustically activated microbubble

where ρ is the density of the fluid ($1,000 \text{ kg m}^{-3}$), σ is the surface tension of water (0.0728 N m^{-1}), κ is the polytropic exponent (1.4) for a bubble containing air (Crum 1983), p_o is the hydrostatic liquid pressure (101.325 kPa), and a is the radius of the bubble at an equilibrium state. Vigorous streaming phenomenon near the bubble interface occurs when the bubbles are driven at their natural frequency. The streaming phenomenon increases the mass transport across the fluidic interface, resulting in fast and homogenous mixing.

3 Experimental details

The PDMS microchannel with pre-designed grooves on the sidewall was fabricated using standard soft lithography

and mold replica technique (Xia and Whitesides 1998). The channel had a width of 240 μm , a depth of 155 μm , and a length of 1.2 cm. The PDMS containing the channel was peeled off from the silicon mold, and inlets and outlets were drilled by a silicon carbide drill bit. It was activated with oxygen plasma and bonded onto a Petri dish. A piezo transducer (model no. 273-073, RadioShack) was bonded using epoxy (Devcon 2 Ton Epoxy) onto the same Petri dish, and placed adjacent to the PDMS microchannel. Before running any experiments, we allowed the epoxy to completely cure for 24 h. We used plastic Petri dishes over glass substrates since they provide better coupling of acoustic energy than glass. Lastly, polyethylene tubings (Becton Dickinson) were inserted to the drilled inlets and outlets of the channel and connected to the syringe pump (KDS 210, KD scientific, Holliston, MA, USA). When the piezo transducer was activated by a function generator (Hewlett Packard 8116A), acoustic waves were generated and propagated into the channel. The driving voltage was held constant at 8 V_{pp} in all the experiments. The whole setup was mounted on a Nikon TE-2000U optical microscope stage.

4 Results

4.1 Bubble oscillation induced by acoustic waves

To demonstrate the oscillation of the bubble membranes, deionized water was injected into the channel to trap air bubbles. Figure 2a shows a trapped bubble within the rectangular grooves in the absence of acoustic waves. The membranes of the air bubbles were acoustically oscillated at their natural frequency. Maximal membrane oscillation of approximately 8 μm was observed at a driving frequency of 81.4 kHz. Figure 2b shows the bubble oscillation in the presence of acoustic waves. A standing wave was generated at the bubble interface. Maximal membrane oscillation of approximately 8 μm was observed at a driving frequency of 81.4 kHz. The bubble oscillation process is more evident in Video 2 in the Supporting Information. Based on Eq. 1, the theoretical natural frequency of a spherical air bubble with a radius of 45 μm was calculated to be 73.4 kHz. The discrepancy between the experimental and the calculated natural frequencies can be attributed to the non-spherical shape of the air bubbles trapped within the sidewall grooves.

4.2 Streaming phenomenon due to bubble oscillations

To demonstrate the recirculation flow pattern inside the channel due to acoustic streaming induced by bubble

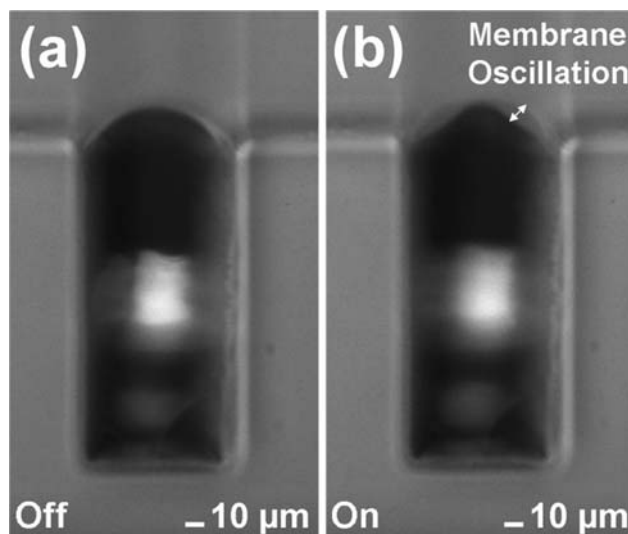


Fig. 2 Optical image of an air bubble trapped inside the groove **a** in the absence of acoustic waves and **b** in the presence of acoustic waves, which induce the bubble membrane to oscillate at its natural frequency

oscillation, a solution containing dragon green fluorescent beads of diameter 1.9 μm (Bangs Laboratory) was injected into the channel inlet. Figure 3a shows the flow pattern of fluorescent bead solution prior to exciting the microbubbles. Once activated, bubbles induced strong acoustic streaming phenomena (Fig. 3b). The streaming effects drastically perturbed bulk laminar flow and enhanced the mass transport across the centerline of the channel thus making fast and homogenous mixing possible.

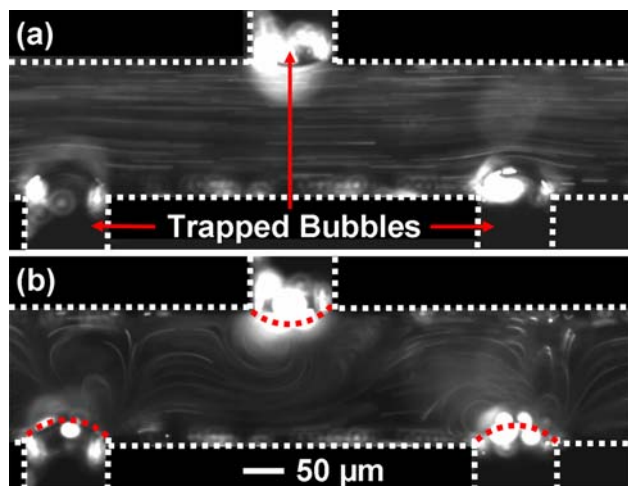


Fig. 3 Characterization of the flow pattern with/without acoustic streaming. **a** In the absence of acoustic waves, laminar flow pattern was observed in a solution containing fluorescent beads (diameter: 1.9 μm). **b** When acoustic waves were applied, streaming was developed in the liquid around the bubbles

4.3 Mixing visualization

To manifest mixing of two fluids inside the channel, deionized water and ink were injected into each inlet at four different flow rates (3, 6, 9, 12 $\mu\text{l}/\text{min}$), resulting in trapped air bubbles within the sidewall grooves. Figure 4a shows the side-by-side laminar flow of co-injected fluids along the channel prior to acoustic excitation at 6 $\mu\text{l}/\text{min}$. A clear fluidic interface was observed due to the poor mixing. The air bubbles were subsequently excited at the natural frequency, and the oscillations of the bubbles led to vigorous streaming phenomena. The acoustic streaming phenomena rapidly interchanged fluids across the channel thus enhanced the mass transport between ink and water and resulted in fast and homogenized mixing (Fig. 4b). The mixing can be repeatedly turned on and off as we switch on/off the acoustic transducer, as shown in Video 3 in the Supporting Information.

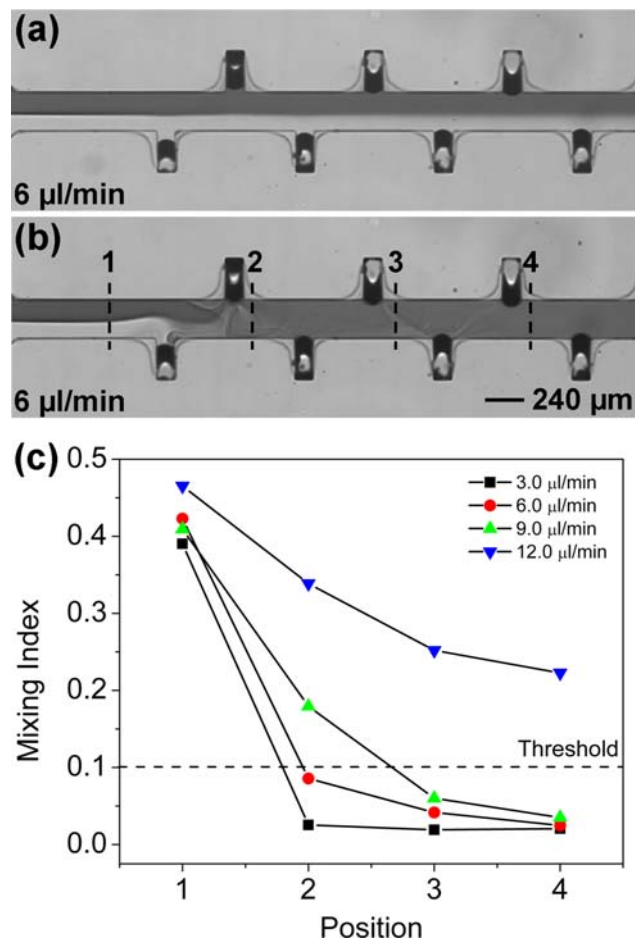


Fig. 4 Characterization of the mixing performance. **a** Laminar flow of deionized water and ink in the absence of acoustic waves. **b** Well mixed deionized water and ink along the channel due to bubble streaming induced by acoustic waves. **c** Plots of mixing indexes at different positions along the microchannel at different flow rates. The x axis indicates different positions shown in **b**

4.4 Mixing quantification

Homogenous mixing was quantified by calculating the mixing index of fluids. The gray-scale value (a good indicator for the ink concentration) was extracted from the image using the image analysis package, image J (NIH, Bethesda, MD, USA), at different locations of the channel (indicated as Positions 1, 2, 3, and 4 in Fig. 4b). The mixing index is the standard deviation of normalized gray scale values. A mixing index of 0.5 indicates unmixed fluids, and a mixing index of 0.0 indicates complete mixing. We chose a mixing index of 0.1 as threshold for acceptable mixing. Mixing indexes at different positions along the channel at four different flow rates were studied. We arbitrarily chose the mixing index less than 0.1 as the criteria for acceptable mixing. At a flow rate of 3 $\mu\text{l}/\text{min}$, mixing index of 0.025 at position 2 was achieved, which suggests excellent mixing of the two fluids (Fig. 4c). At a higher flow rate, 6 $\mu\text{l}/\text{min}$, close-to-perfect mixing (mixing index: 0.084) was achieved after passing through the second bubble as shown in Fig. 4c. At 9 $\mu\text{l}/\text{min}$, acceptable mixing (mixing index = 0.06) was only observed after passing position 3, and the mixing index at position 2 was 0.179. When the flow rate was increased to 12 $\mu\text{l}/\text{min}$, no significant mixing was observed (Fig. 4c) even after passing position 4. The threshold flow rate for which we achieved mixing index of less than 0.1 after passing position 2 (right after the first two bubbles) was 6 $\mu\text{l}/\text{min}$. The average mixing time, τ_s , was estimated by using

$$\tau_s = L_{\text{mix}}/v_{\text{avg}}, \quad (2)$$

where L_{mix} is the distance ($\sim 650 \mu\text{m}$) from the unmixed to completely mixed region, and v_{avg} was the average fluid velocity estimated by dividing the total flow rate (12 $\mu\text{l}/\text{min}$) of the injected liquids by the cross-sectional area of the channel (240 by 155 μm). The mixing time was thus calculated to be less than 120 ms. We believe that with optimization of parameters such as the bubble encapsulation geometry or the natural frequency, it is possible to further reduce the mixing time.

5 Conclusion

In conclusion, we report a microfluidic mixer based on bubble-induced acoustic streaming effects. The injection of fluid into the microchannel results in trapped air bubbles in the sidewall grooves. As these air bubbles are acoustically excited at their natural frequencies, vigorous streaming phenomena are induced. This streaming breaks the laminar fluid interface, enhances the mass transport between the two fluids, and thus enables fast and homogenous mixing.

Effective mixing is observed across the width of the channel. Furthermore, the mixing time is calculated to be less than 120 ms. Due to its simple design, strong performance, and fast speed, this technique could be used in a wide variety of “lab-on-chip” applications that require fast and homogenous mixing.

Acknowledgments Authors thank Madineh Sarvestani, Thomas Walker, and Aitan Lawit for helpful discussion and Tristan Tabouillot for assistance in experiments. This research was supported by National Science Foundation (ECCS-0824183 and ECCS-0801922) and the Penn State Center for Nanoscale Science (MRSEC). Components of this work were conducted at the Penn State node of the NSF-funded National Nanotechnology Infrastructure Network.

References

- Chang CC, Yang RJ (2007) Electrokinetic mixing in microfluidic systems. *Microfluid Nanofluid* 3:501–525
- Chen H, Meiners JC (2004) Topological mixing on a microfluidic chip. *Appl Phys Lett* 84:2193–2195
- Crum LA (1983) The polytropic exponent of gas contained within air bubbles pulsating in liquid. *J Acoust Soc Am* 73:116–120
- Erickson D, Li D (2002) Influencing of surface heterogeneity on electrokinetically driven microfluidic mixing. *Langmuir* 18:1883–1892
- Frommelt T, Kostur M, Wenzel-Schäfer M, Talkner P, Hänggi P, Wixforth A (2008) Microfluidic mixing via acoustically driven chaotic advection. *Phys Rev Lett* 100:34502
- Hellman AN, Rau KR, Yoon HH, Bae S, Palmer JF, Phillips KS, Allbritton NL, Venugopalan V (2007) Laser-induced mixing in microfluidic channel. *Anal Chem* 79:4484–4492
- Ho CM, Tai YC (1998) Micro-electro-mechanical systems (MEMS) and fluid flows. *Annu Rev Fluid Mech* 30:579–612
- Lam YC, Chen X, Yang C (2005) Depthwise averaging approach to cross-stream mixing in a pressure-driven microchannel flow. *Microfluid Nanofluid* 1:218–226
- Law NS, Khoo BC (2002) Transport across a turbulent air–water interface. *AIChE J* 48:1856–1868
- Lee CY, Lee GB, Fu LM, Lee KH, Yang RJ (2004) Electrokinetically driven active micro-mixers utilizing zeta potential variation induced by field effect. *J Micromech Microeng* 14:1390–1398
- Lee YK, Shih C, Tabeling P, Ho CM (2007) Experimental study and nonlinear dynamic analysis of time-periodic micro chaotic mixers. *J Fluid Mech* 575:425–448
- Leighton TG (1994) *The acoustic bubble*. Academic Press, London
- Li D (2008) *Encyclopedia of microfluidics and nanofluidics*. Springer, Berlin
- Lin YC, Chung YC, Wu CY (2007) Mixing enhancement of the passive microfluidic mixer with J-shaped baffles in the tee channel. *Biomed Microdevices* 9:215–221
- Liu RH, Yang J, Pindera MZ, Athavale M, Grodzinski P (2002) Bubble-induced acoustic micromixing. *Lab Chip* 2:151–157
- Mao X, Waldeisen JR, Huang TJ (2007a) “Microfluidic drifting”-implementing three-dimensional hydrodynamic focusing with a single-layer planar microfluidic device. *Lab Chip* 7:1260–1262
- Mao X, Waldeisen JR, Huang TJ (2007b) Hydrodynamically tunable optofluidic cylindrical microlens. *Lab Chip* 7:1303–1308
- Marmottant P, Hilgenfeldt S (2004) A bubble-driven microfluidic transport element for bioengineering. *Proc Natl Acad Sci USA* 101:9523–9527
- Ottino JM, Wiggins S (2004) Designing optimal micromixers. *Science* 305:485–486
- Park HY, Qiu X, Rhoades E, Korch J, Kwok LW, Zipfel WR, Webb WW, Pollack L (2006) Achieving uniform mixing in a microfluidic device: hydrodynamic focusing prior to mixing. *Anal Chem* 78:4465–4473
- Sannomiya T, Hafner C, Vörös J (2008) In situ sensing of single binding events by localized surface Plasmon resonance. *Nanolett* 8(10):3450–3455
- Shi J, Mao X, Ahmed D, Colletti A, Huang TJ (2008) Focusing microparticles in a microfluidic channel with standing surface acoustic waves (SSAW). *Lab Chip* 8:221–223
- Song H, Ismagilov RF (2003) Millisecond kinetics on a microfluidic chip using nanoliters of reagents. *J Am Chem Soc* 125:14613–14619
- Stroock AD, Dertinger SKW, Ajdari A, Mezic I, Stone HA, Whitesides GM (2002) Chaotic mixers for microchannel. *Science* 295:647–651
- Tho P, Manasseh R, Ooi A (2007) Cavitation microstreaming patterns in single and multiple bubbles systems. *J Fluid Mech* 576:191–233
- Tsai JH, Lin L (2002) Active microfluidic mixer and gas bubble filter driven by thermal bubble micropump. *Sens Actuators A* 97:665–671
- Whitesides GM (2006) The origins and the future of microfluidics. *Nature* 442:368–373
- Wu Z, Li D (2008) Micromixing using induced-charge electrokinetic flow. *Electrochim Acta* 53:5827–5835
- Xia Y, Whitesides GM (1998) Soft lithography. *Annu Rev Mater Sci* 28:153–184
- Yaralioglu GG, Wygant IO, Marentis TC, Khuri-Yakub B (2004) Ultrasonic mixing in microfluidic channels using integrated transducers. *Anal Chem* 76:3694–3698